THE EFFECTS OF ANISOTROPY ON THE NONLINEAR BEHAVIOR OF BRIDGED CRACKS IN LONG STRIPS

H. A. Luo† and R. Ballarini‡

† Department of Engineering Mechanics, Shanghai Jiao Tong University, Shanghai 200030,
China ; and ‡ Department of Civil Engineering, Case Western Reserve University, Cleveland,
Ohio 44106, U.S.A.

ABSTRACT

THIS PAPER PRESENTS a model which can be used to predict the two-dimensional nonlinear behavior of bridged cracks in orthotropic strips. The results obtained using a singular integral equation formulation which incorporates the anisotropy rigorously show that, although the effects of anisotropy are significant, the nondimensional quantities employed by Cox and Marshall (*Acta Metall.* **39**, 579–589, 1991) can generate nearly universal results (R-curves, for example) for different levels of relative anisotropy. The role of composite constituent properties in the behavior of bridged cracks is clarified in this paper.

1. INTRODUCTION

THE BRIDGING of cracks by fibers is an important toughening mechanism in fiber reinforced brittle matrix composites (BMC). Similar characteristics are shared by ductile matrix composites (DMC) with weak interfaces upon cyclic loading (EVANS, 1991). This fact has led to a significant amount of research in the area of stress analysis of bridged cracks. The results calculated with the models presented by MARSHALL *et al.* (1985), MARSHALL and COX (1987), COX and MARSHALL (1991), COX (1991) and BALLARINI and MUJU (1993) have provided a good understanding of the fracture mechanics of bridged cracks in *finite* specimens. In all these models, excluding the orthotropic finite element model used by Ballarini and Muju, the anisotropy which is inherent in fiber reinforced composites was incorporated in an approximate way which may or may not provide an accurate account of its effects.

The integral equation model for a bridged crack in a finite specimen developed by Cox and co-workers can be summarized as follows. A fictitious line load P per unit width of crack front was placed on one crack surface at position x measured normal to the crack front. Using Castigliano's theorem the crack opening displacement (COD) $u(x)$ was determined as $u(x) = \lim_{P \to 0} \partial W / \partial P$, where W is the elastic strain energy of the system per unit width of crack front. This energy was then written in terms of the crack length a, strain energy release rate $\mathscr{G}$ and stress intensity factor K, i.e. $W = \int_0^a \mathscr{G} \, \mathrm{d}a' = \int_0^a K^2 / E' \, \mathrm{d}a'$. In this equation E' is given, for an orthotropic material with a plane stress crack parallel to the principal material axis ox_1-axis, as $1/E' = \sqrt{l_{11} l_{22}/2} \{\sqrt{l_{22}/l_{11}} + (2l_{12} + l_{66})/2l_{11}\}^{1/2}$, where the l_{ij} are compliance

coefficients which enter the inverse Hooke's law, as will be explained in the next section. Cox and Marshall made the following approximation. They expressed the stress intensity factor K in terms of the Green's function $G(x, a', w)$ for the *isotropic* material, where w is a relevant characteristic length which introduces finite geometry. The representation $K = 2 \int_0^{a'} G(x, a', w)\sigma(x)\,dx$, where $\sigma(x)$ is the traction on the crack surface, leads to the integral equation $u(x) = (4/E') \int_x^a da' \{ \int_0^a G(x', a', w)\sigma(x)\,dx' \} \times G(x, a', w)$, which they solved numerically. This integral equation can be more directly derived using the weight function technique (Bueckner, 1970). Thus, the Green's function $G(x, a', w)$ can also be referred to as the Bueckner weight function. This model, by neglecting the dependency of the Green's function on the compliance coefficients, leads to the result that the COD is inversely proportional to E'. Moreover, normalization of this integral equation leads to the so-called bridging length scale a_n, that is associated with a fully bridged crack in an infinitely extended material. A crack length $a \ll a_n$ is considered short in the sense that its bridging zone is still developing. For these short fully bridged cracks the forces in the fibers are relatively small, since the crack opening displacements are small. Hence the fibers do not shield the crack tip significantly, and the stress required to propagate the matrix crack is inversely proportional to the square root of the crack length, as for the monolithic matrix. For $a \gg a_n$ the crack is termed long, because the bridging zone has fully developed and a steady state is reached for matrix cracking (the stress required to propagate the matrix crack is independent of crack length).

The authors have recently learned of the significant contribution to the understanding of the role of material orthotropy in fracture specimens for composites made by Suo *et al.* (1991). They found a spatial rescaling that could be used to reduce boundary value problems (BVP) involving orthotropic materials to equivalent problems in materials with cubic symmetry. Under certain conditions the cubic-symmetric materials may be approximated by isotropic materials. Therefore the rescaling technique can be used in conjunction with existing isotropic material solutions to construct approximate orthotropic material solutions. These spatial rescaling relations, which will be discussed subsequently, were used by Bao *et al.* (1992) in their analysis of commonly used fracture specimens to investigate the interplay between material anisotropy and finite geometry. In their finite element method analysis the role of orthotropy in fiber bridging phenomena was not considered.

The work presented in this paper was initiated to investigate the effects of relative anisotropy on the behavior of *bridged cracks* in long strips so that the assumption used in the aforementioned analyses of bridged cracks could be assessed. Moreover, an efficient and highly accurate analytical model based on dislocation theory was sought that will facilitate the analysis of experiments conducted on beam specimens. The results obtained using a singular integral equation formulation which incorporates rigorously the effects of orthotropy, show that the weight function $G(x', a', w)$ depends not only on E' but also other stiffness coefficients. However, the numerical calculations presented in this paper indicate that for the unbridged cracks in different orthotropic strips the CODs are indeed approximately inversely proportional to their values of E'. A wide range of computations for the nonlinear behavior of bridged cracks also supports the adoption of simple approximate weight functions which are derived for the corresponding isotropic specimen. These results generalize the conclusions made

by Bao *et al.* to fiber-bridged cracks in long strips. Evidently, this conclusion will facilitate the analysis of *R*-curves for bridged cracks in orthotropic beam specimens.

2. FORMULATION

Consider an infinite orthotropic plate whose principal material axes coincide with the coordinate axes. A unit dislocation with Burgers vector $b_x = 1$ is embedded at $P(0, y_0)$. The stresses in the plate are (MILNE-THOMSON, 1960)

$$\sigma_{xx}^{(1)} = \tfrac{1}{2} \operatorname{Re}\left[\frac{A_1\lambda_1^2}{z_1} + \frac{A_2\lambda_2^2}{z_2}\right], \quad \sigma_{yy}^{(1)} = \tfrac{1}{2} \operatorname{Re}\left[\frac{A_1}{z_1} + \frac{A_2}{z_2}\right],$$

$$\sigma_{xy}^{(1)} = -\tfrac{1}{2} \operatorname{Re}\left[\frac{A_1\lambda_1}{z_1} + \frac{A_2\lambda_2}{z_2}\right], \tag{1}$$

where

$$z_1 = x + \lambda_1(y - y_0), \quad z_2 = x + \lambda_2(y - y_0), \tag{2}$$

λ_1 and λ_2 are two roots of the characteristic equation

$$l_{11}\lambda^4 + (2l_{12} + l_{66})\lambda^2 + l_{22} = 0 \tag{3}$$

with $\operatorname{Im}(\lambda_1) \geqslant \operatorname{Im}(\lambda_2) > 0$, $\lambda_3 = -\lambda_1$, $\lambda_4 = -\lambda_2$. The l_{ij} are the anisotropic compliance coefficients which enter the inverse Hooke's law,

$$\begin{pmatrix} \varepsilon_{xx} \\ \varepsilon_{yy} \\ 2\varepsilon_{xy} \end{pmatrix} = \begin{pmatrix} l_{11} & l_{12} & 0 \\ l_{12} & l_{22} & 0 \\ 0 & 0 & l_{66} \end{pmatrix} \begin{pmatrix} \sigma_{xx} \\ \sigma_{yy} \\ \sigma_{xy} \end{pmatrix}. \tag{4}$$

In (1), the constants A_1 and A_2 are determined by

$$\begin{cases} p_1 A_1 + p_2 A_2 - \bar{q}_1 \bar{A}_1 - \bar{q}_2 \bar{A}_2 = 2/\pi i, \\ \delta_1 A_1 + \delta_2 A_2 - \bar{\gamma}_1 \bar{A}_1 - \bar{\gamma}_2 \bar{A}_2 = 0, \end{cases} \tag{5}$$

where

$$p_1 = l_{12} + l_{11}\lambda_1^2 + i(l_{22} + l_{12}\lambda_1^2)/\lambda_1,$$

$$p_2 = l_{12} + l_{11}\lambda_2^2 + i(l_{22} + l_{12}\lambda_2^2)/\lambda_2,$$

$$\bar{q}_1 = l_{12} + l_{11}\bar{\lambda}_1^2 + i(l_{22} + l_{12}\bar{\lambda}_1^2)/\bar{\lambda}_1,$$

$$\bar{q}_2 = l_{12} + l_{11}\bar{\lambda}_2^2 + i(l_{22} + l_{12}\bar{\lambda}_2^2)/\bar{\lambda}_2,$$

$$\delta_1 = (1 + i\lambda_1)/2, \quad \delta_2 = (1 + i\lambda_2)/2,$$

$$\gamma_1 = (1 - i\lambda_1)/2, \quad \gamma_2 = (1 - i\lambda_2)/2. \tag{6}$$

The first equation in (5) represents the necessary displacement jump condition, while the second represents zero net force on the dislocation.
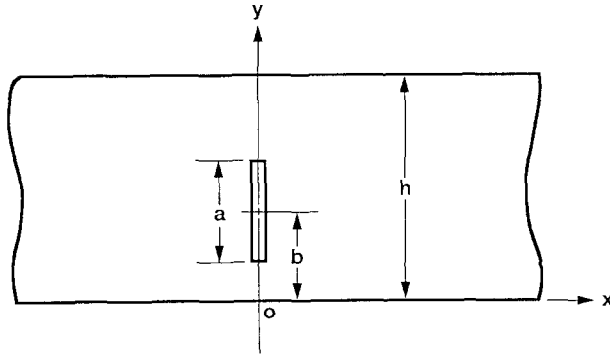
FIG. 1. Configuration of the cracked strip.

When the dislocation is located in an orthotropic strip (Fig. 1), an additional solution must be superposed to satisfy the traction free boundary conditions on the surfaces $y = 0$ and $y = h$. The stresses from the additional solution, denoted by superscript (2), must satisfy

$$\sigma_{yy}^{(2)}(x, 0) = -\sigma_{yy}^{(1)}(x, 0), \quad \sigma_{xy}^{(2)}(x, 0) = -\sigma_{xy}^{(1)}(x, 0),$$

$$\sigma_{yy}^{(2)}(x, h) = -\sigma_{yy}^{(1)}(x, h), \quad \sigma_{xy}^{(2)}(x, h) = -\sigma_{xy}^{(1)}(x, h). \tag{7}$$

This part of the solution can be determined using Fourier transformation techniques. Its displacement components are expressed as

$$u^{(2)}(x, y) = \frac{2}{\pi} \int_0^\infty U(\xi, y) \sin \xi x \, dx,$$

$$v^{(2)}(x, y) = \frac{2}{\pi} \int_0^\infty V(\xi, y) \cos \xi x \, dx, \tag{8}$$

with

$$U(\xi, y) = \sum_{j=1}^4 B_j(\xi) \exp (s_j \xi y),$$

$$V(\xi, y) = \sum_{j=1}^4 d_j B_j(\xi) \exp (s_j \xi y), \tag{9}$$

where

$$d_j = [\beta_2 s_j^3 - (\beta_1 \beta_2 - \beta_3^2) s_j]/\beta_3, \tag{10}$$

and the s_j $(j = 1, 2, \ldots, 4)$ are the roots of the equation

$$s^4 + \frac{\beta_3^2 - \beta_1 \beta_2 - 1}{\beta_2} s^2 + \frac{\beta_1}{\beta_2} = 0. \tag{11}$$

In (10) and (11)

$$\beta_1 = b_{11}/G_{12}, \quad \beta_2 = b_{22}/G_{12}, \quad \beta_3 = 1 + b_{12}/G_{12}, \tag{12}$$

where the b_{ij} and G_{12} are the stiffness coefficients of the material:

$$\begin{pmatrix} \sigma_{xx} \\ \sigma_{yy} \\ \sigma_{xy} \end{pmatrix} = \begin{pmatrix} b_{11} & b_{12} & 0 \\ b_{12} & b_{22} & 0 \\ 0 & 0 & G_{12} \end{pmatrix} \begin{pmatrix} \varepsilon_{xx} \\ \varepsilon_{yy} \\ 2\varepsilon_{xy} \end{pmatrix}. \tag{13}$$

Using condition (7), the coefficients $B_j(\xi)$ $(j = 1, 2, \ldots, 4)$ can be determined by solving the set of linear equations given in the Appendix.

Along the y-axis the resultant stress σ_{xx} in the strip is

$$\sigma_{xx}(0, y) = \frac{\kappa}{y_0 - y} + G(y, y_0) \tag{14}$$

with

$$G(y, y_0) = \frac{2b_{11}}{\pi} \sum_{j=1}^{4} \int_0^\infty B_j(\xi) \, \mathrm{e}^{y_j \xi y} \, \mathrm{d}\xi + \frac{2b_{12}}{\pi} \sum_{j=1}^{4} d_j s_j \int_0^\infty B_j(\xi)\xi \, \mathrm{e}^{y_j \xi y} \, \mathrm{d}\xi,$$

$$\kappa = -\operatorname{Re}(A_1 \lambda_1 + A_2 \lambda_2)/2. \tag{15}$$

The stiffness parameter κ plays a crucial role in defining the level of anisotropy of a given material system. After comparing it with the relevant quantities E' and A which are adopted by Cox and Marshall (1991) and Budiansky and Amazigo (1989), respectively, it is found that

$$\kappa = \frac{E'}{4\pi} = \frac{AE_{11}}{4\pi(1 - v_m^2)} \tag{16}$$

where v_m is the matrix Poisson's ratio and E_{11} the longitudinal composite Young's modulus. Because the crack is now perpendicular to the x-axis, in (16)

$$\frac{1}{E'} = \left(\frac{l_{11}l_{22}}{2}\right)^{1/2} \left[\left(\frac{l_{11}}{l_{22}}\right)^{1/2} + \frac{2l_{12} + l_{66}}{2l_{22}}\right]^{1/2}. \tag{17}$$

This quantity was first introduced by Sih and Liebowitz (1968).

With (17) the relative in-plane orthotropy is specified through three ratios: l_{22}/l_{11}, l_{12}/l_{11} and l_{66}/l_{11}. Suo (1990a, b) introduced two parameters

$$\lambda = \frac{l_{11}}{l_{22}}, \quad \rho = \frac{2l_{12} + l_{66}}{2\sqrt{l_{11}l_{22}}} \tag{18}$$

as the only two parameters needed to quantify the level of orthotropy. $\lambda = \rho = 1$ for isotropic solids and $\lambda = 1$ for solids with cubic symmetry. Using Lekhnitskii's formalism (1981) he showed that in simply-connected sheets with traction prescribed on the boundary, the governing equation for the Airy stress function can be written as

$$\frac{\partial^4 U}{\partial x^4} + 2\rho\sqrt{\lambda}\,\frac{\partial^4 U}{\partial x^2\,\partial y^2} + \lambda\,\frac{\partial^4 U}{\partial y^4} = 0. \tag{19}$$

This suggests that the stresses depend on material properties only through ρ and λ. Furthermore, by rescaling the x-axis by $\xi = \lambda^{1/4}x$ the λ dependence can be extracted explicitly, so that in the transformed plane the stresses depend only on ρ, i.e.

$$\frac{\partial^4 U}{\partial \xi^4} + 2\rho\,\frac{\partial^4 U}{\partial \xi^2\,\partial y^2} + \frac{\partial^4 U}{\partial y^4} = 0. \tag{20}$$

Obviously, solution to BVP for the class of materials obeying $\rho = 1$ $(\lambda \neq 1)$ can be constructed from the solution to the corresponding BVP for the isotropic material. It can be shown that

$$\frac{1}{E'} = l_{22}\sqrt{\frac{\lambda^{3/2}(1+\rho)}{2}} \tag{21}$$

for a crack in the y-direction. The parameters λ and ρ will be considered in subsequent calculations.

Consider a cracked strip shown in Fig. 1 and introduce parameters t and τ such that $y = b + at/2$ and $y_0 = b + a\tau/2$. The discrete dislocation is replaced with a distribution of dislocations

$$B_x(\tau) \equiv -\frac{2}{a}\frac{\partial}{\partial \tau}[u(0^+, \tau) - u(0^-, \tau)]. \tag{22}$$

This representation enables one to write the following singular integral equation for the traction boundary condition along the crack, with expression (14) being the appropriate kernel:

$$\int_{-1}^{1} \frac{B_x(\tau)}{\tau - t}\,d\tau + \int_{-1}^{1} K(t, \tau)B_x(\tau)\,d\tau = -q(t), \tag{23}$$

where $K(t, \tau)$ is the regular part of the kernel

$$K(t, \tau) = \frac{a}{2\kappa}\,G(b + at/2, b + a\tau/2), \tag{24}$$

and the loading term is given by

$$q(t) = \frac{1}{\kappa}[\sigma_A(t) - p(t)]. \tag{25}$$

Here $\sigma_A(t)$ is the stress caused by the applied load in the crack-free strip and $p(t)$ is the closing stress of the bridging fibers. In general, $p(t) = p(u(t))$ where $u(t)$ is the crack opening displacement at t. For internal cracks, the crack closure condition

$$\int_{-1}^{1} B_x(\tau)\,d\tau = 0 \tag{26}$$

should be supplemented to (23). The square root stress singularity at crack tips is modeled by expressing $B_x(\tau)$ as

$$B_x(\tau) = \phi(\tau)/\sqrt{1 - \tau^2} \tag{27}$$

for internal cracks and

$$B_x(\tau) = \phi(\tau)/\sqrt{1 - \tau} \tag{28}$$

for edge cracks, where $\phi(\tau)$ is a regular function.

It is important to note that unlike the isotropic case, where the kernel of the singular integral equation is independent of the elastic constants, the kernel which appears in (23) depends on the ratios E_{22}/E_{11}, G_{12}/E_{11} and v_{12} for the plane stress case and E_{22}/E_{11}, E_{33}/E_{11}, G_{12}/E_{11}, v_{12}, v_{13} and v_{23} for the plane deformation case. Nevertheless, from a viewpoint of the orthotropy rescaling, in the transformed ξy-plane the stress field for a unit dislocation $b_x = 1$ embedded in a long strip is determined by governing equation (20). The corresponding boundary conditions are

$$\frac{\partial^2 U}{\partial \xi^2} = 0, \quad \frac{\partial^2 U}{\partial \xi \, \partial y} = 0 \tag{29}$$

at $y = 0$ and $y = h$. On the dislocation, the zero net force condition and the displacement jump condition are (BAO et al., 1992)

$$\left[\frac{\partial U}{\partial y}\right]_L = 0, \quad \left[\frac{\partial U}{\partial \xi}\right]_L = 0, \tag{30}$$

and

$$\left[\frac{\partial \chi}{\partial y}\right]_L = 4\pi\kappa\sqrt{\frac{1 + \rho}{2}}, \quad \left[\frac{\partial \chi}{\partial \xi}\right]_L = 0, \tag{31}$$

respectively, where the symbol $[\ ]_L$ denotes the increment received on passing once round a closed curve enclosing the dislocation and χ is the auxiliary function defined by

$$\frac{\partial^2 \chi}{\partial \xi \, \partial y} = \frac{\partial^2 U}{\partial \xi^2} + \frac{\partial^2 U}{\partial y^2}, \quad 2(1 - \rho)\frac{\partial^2 U}{\partial \xi \, \partial y} = \frac{\partial^2 \chi}{\partial \xi^2} + \frac{\partial^2 \chi}{\partial y^2}. \tag{32}$$

Therefore, the kernel of (23), which is equal to $(1/\kappa)(\partial^2 U/\partial y^2)$, depends on elastic constants only through the nondimensional parameters λ and ρ. Moreover, because in Fig. 1 there is no characteristic length in the x-direction the kernel actually is a function of ρ only.

The above integral equations are solved numerically. By approximating $\phi(t)$ as piecewise quadratic polynomials, (23) and (26) are reduced to:

$$\sum_{j=1}^{n} M_{ij}\phi(\tau_j) = -\frac{1}{\kappa}[\sigma_A(t_i) - p(u(t_i))] \tag{33}$$

where τ_j is the integral point, t_i is the collocation point and the matrix element M_{ij}

consists of the weights given in GERASOULIS (1982). For edge cracks $i = 1, 2, \ldots, n$, and for internal cracks $i = 1, 2, \ldots, n-1$ with the nth equation

$$\sum_{j=1}^{n} M_{nj} \phi(\tau_j) = 0 \tag{34}$$

coming from (26). In the following discussion, we only consider edge-cracked and center-cracked strips.

Equation (33) represents a set of nonlinear equations for the unknown dislocation distribution. A more efficient iteration procedure is obtained by deriving a compliance matrix, as outlined in BALLARINI (1986).

From (33) and (34),

$$\phi(\tau_j) = -\frac{1}{\kappa} \sum_{k=1}^{n} N_{jk}[\sigma_\Lambda(\tau_k) - p(u(\tau_k))] \quad (j = 1, 2, \ldots, n) \tag{35}$$

where $N = M^{-1}T$ with M^{-1} denoting the inverse of matrix M, and T is an $n \times n$ matrix which transforms the coordinates from the integral points to the collocation points. Following BALLARINI (1986), by substituting (35) into (28) and integrating $B_x(\tau)$ from τ_j to 1, (35) is cast in the form:

$$u(\tau_j) = \frac{a}{\kappa} \sum_{k=1}^{n-1} C_{jk}[\sigma_\Lambda(\tau_k) - p(u(\tau_k))] \quad (j = 1, 2, \ldots, n-1) \tag{36}$$

where the matrix C is known as the compliance matrix of the crack which relates the stress on the crack face with the crack opening displacement. Thus, a system of nonlinear algebraic equations for crack opening displacement $u(\tau_j)$ is obtained.

The total stress intensity factor which includes the fiber shielding effects is

$$K_T = -\eta\kappa\pi\sqrt{\pi a}\phi(1)$$
$$= \eta\pi\sqrt{\pi a} \sum_{k=1}^{n} N_{nk}[\sigma_\Lambda(\tau_k) - p(u(\tau_k))], \tag{37}$$

while the so-called shielding stress intensity factor is given by

$$K_F = \eta\pi\sqrt{\pi a} \sum_{k=1}^{n} N_{nk} p(u(\tau_k)). \tag{38}$$

Here $\eta = 1$ for edge cracks and $\eta = 1/\sqrt{2}$ for center cracks, respectively. It is obvious that $K_T = K_\Lambda - K_F$ where K_Λ is the stress intensity factor due to applied load only.

3. RESULTS AND DISCUSSION

Zero fiber bridging

To check the numerical procedure, calculations were first performed for the case of zero fiber bridging stress. The computed stress intensity factors and crack mouth opening displacement (CMOD) for uniform tension and bending, for various values of relative orthotropy and crack length, are practically the same as those reported by

TABLE 1. *Normalized stress intensity factor vs orthotropy rescaling parameters λ and ρ for zero fiber bridged edge cracks*

| | | $K/\sigma_x \sqrt{\pi a/2}$ | | | | | |
| | | | | | ρ | | |
λ	a/h	0	1	2	3	4	5
	0.1	1.247	1.190	1.167	1.154	1.146	1.140
0.2	0.3	1.725	1.661	1.639	1.627	1.620	1.615
	0.5	2.964	2.833	2.783	2.755	2.738	2.726
	0.1	1.247	1.190	1.167	1.154	1.146	1.140
0.6	0.3	1.725	1.661	1.639	1.627	1.620	1.615
	0.5	2.964	2.833	2.783	2.755	2.738	2.726
	0.1	1.247	1.190	1.167	1.154	1.146	1.140
1.0	0.3	1.725	1.661	1.639	1.627	1.620	1.615
	0.5	2.964	2.833	2.783	2.755	2.738	2.726

DELALE and ERDOGAN (1977) and KAYA and ERDOGAN (1980), and are not presented here. Selected results for plane stress edge cracks under uniform tension are presented in Tables 1 and 2 to highlight the significance of material anisotropy.

Tables 1 and 2 show the normalized stress intensity factor $K/\sigma_x\sqrt{\pi a/2}$ and normalized crack mouth opening displacement $[u]E'/2\sigma_x h$, respectively, as functions of the orthotropy rescaling factors λ and ρ. It is observed that for a given crack length, both the quantities are independent of λ and are weak functions of ρ. This is because the kernel of (23) is a function of ρ only. As a result, the parameter ρ will slightly change the proportionality of $[u]$ to $1/E'$. Such effects also exist on the relation between bridging force and relative anisotropy.

The normalized COD profile for a plane stress edge crack of length equal to one

TABLE 2. *Normalized CMOD vs orthotropy rescaling parameters λ and ρ for zero fiber bridged edge cracks*

| | | $[u]E'/2\sigma_x h$ | | | | | |
| | | | | | ρ | | |
λ	a/h	0	1	2	3	4	5
	0.1	0.355	0.309	0.291	0.280	0.273	0.268
0.2	0.3	1.575	1.406	1.342	1.308	1.286	1.271
	0.5	5.499	4.947	4.742	4.633	4.564	4.517
	0.1	0.355	0.309	0.291	0.280	0.273	0.268
0.6	0.3	1.575	1.406	1.342	1.308	1.286	1.271
	0.5	5.499	4.947	4.742	4.633	4.564	4.517
	0.1	0.355	0.309	0.291	0.280	0.273	0.268
1.0	0.3	1.575	1.406	1.342	1.308	1.286	1.271
	0.5	5.499	4.947	4.742	4.633	4.564	4.517

Fig. 2. Normalized COD for zero fiber bridged edge crack with different relative orthotropy.

half the depth of the beam is plotted in Fig. 2 as a function of relative orthotropy which is obtained by keeping the values of $E_{22} = E_{33}$, $G_{12} = E_{22}/2(1 + v_{12})$, $v_{12} = v_{13} = v_{23} = 0.3$ unchanged while varying the value of E_{11} only. For the cases $E_{11}/E_{22} = 1, 2, 5$ and 10, $E'/E_{22} = 1, 1.47, 2.43$ and 3.55, $\lambda = 1, 0.5, 0.2$ and 0.1, and $\rho = 1, 1.63, 2.77$ and 4.02, respectively. It is seen that, though the material anisotropy has significant influence on the COD, the relation between $[u]E'/2\sigma_\infty h$ and y/a is almost independent of the level of relative orthotropy. The largest discrepancy occurs at the crack mouth, but even for $E_{11}/E_{22} = 10$ it is less than 8% compared with the isotropic case.

Initially fully bridged cracks

Results are calculated next for bridging fibers whose strength satisfies a two parameter Weibull distribution and whose sliding is resisted by a constant fricitonal stress τ. The closing stress can be approximated as (Cox and Marshall, 1991)

$$p(u) = f \Sigma U^{1/2} \exp(-U^{(m+1)/2}), \tag{39}$$

where f is the volume fraction of fibers, m is the Weibull modulus and U is the normalized COD:

$$U = u/u_n, \quad u_n = \frac{\Sigma^2 R(1-f)E_m}{4\tau E_f E_{11}},$$

$$\Sigma = \langle s \rangle / \Gamma\left(\frac{m+1}{m+2}\right), \tag{40}$$

with $\langle s \rangle$ the average fiber strength, Γ the gamma function, R the fiber radius, and E_m, E_f and E_{11} the moduli of the matrix, fiber and composite in the fiber direction.

The effects of anisotropy are demonstrated through the specific example of two plane strain orthotropic strips: strip 1, nearly isotropic with bulk properties $E_{11} = 279.6$ GPa, $E_{22} = E_{33} = 253.9$ GPa, $G_{12} = 97.66$ GPa, and
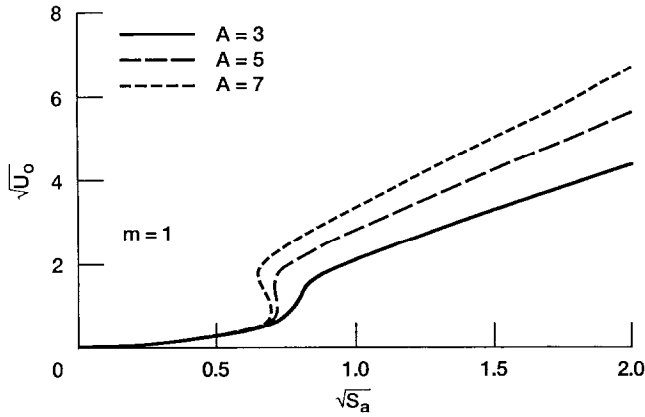
Fig. 3. Normalized crack mouth opening displacement vs normalized loading parameter for bridged Griffith crack.

$v_{12} = v_{13} = v_{23} = 0.3$, and strip 2, with all properties equal to those of strip 1, except $E_{11} = 1398$ GPa. Their rescaling parameters are $\lambda = 0.9163$ and $\rho = 1.086$ for strip 1 and $\lambda = 0.1963$ and $\rho = 3.048$ for strip 2.

For each strip, three different normalized crack lengths were considered: $A = 3, 5, 7$ for uniform tension loading where

$$A = a/a_n, \quad a_n = \frac{\pi \Sigma R(1 - f)E_m E'}{16\tau f E_f E_{11}}. \tag{41}$$

The dimensionless strip width is $H = h/a_n = 10$.

In each analysis the crack length is held fixed as the loading is increased. By controlling the length of the bridged crack, results are obtained which highlight the transition from stable to unstable behavior of the crack. The resulting physical parameters are presented in Figs 3–8. These include the square root of the normalized
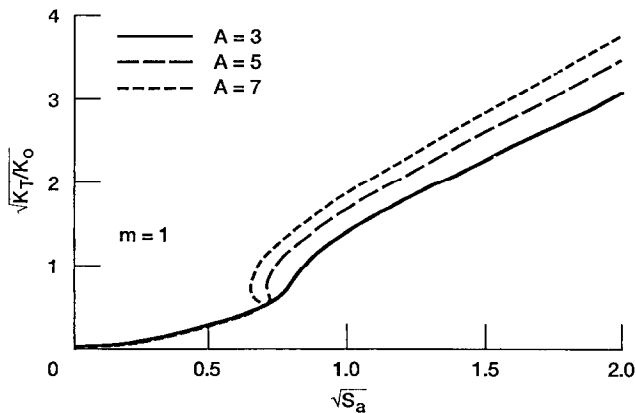
Fig. 4. Normalized total stress intensity factor vs normalized loading parameter for bridged Griffith crack.
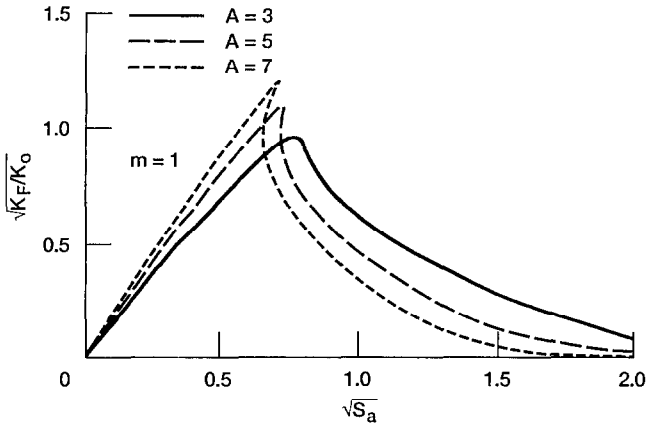
FIG. 5. Normalized shielding stress intensity factor vs normalized loading parameter for bridged Griffith crack.

crack mouth opening displacement $\sqrt{U_0} = \sqrt{u(-1)u_n}$, square roots of the normalized total and shielding stress intensity factors $\sqrt{K_T/K_0}$ and $\sqrt{K_F/K_0}$ as functions of normalized loading parameter $\sqrt{S_a}$, where

$$K_0 = 2f\Sigma\sqrt{2a_n/3\pi}, \tag{42}$$

$S_a = \sigma_x/f\Sigma$ for uniform tension under stress σ_x.

It should be noted that the nondimensional variables used in equations (39)–(42) were defined by COX and MARSHALL (1991). They are adopted in the present analysis to drive home the point whether this set of nondimensional parameters are sufficient to predict the behaviour of bridged cracks in composite materials which possess different levels of anisotropy.
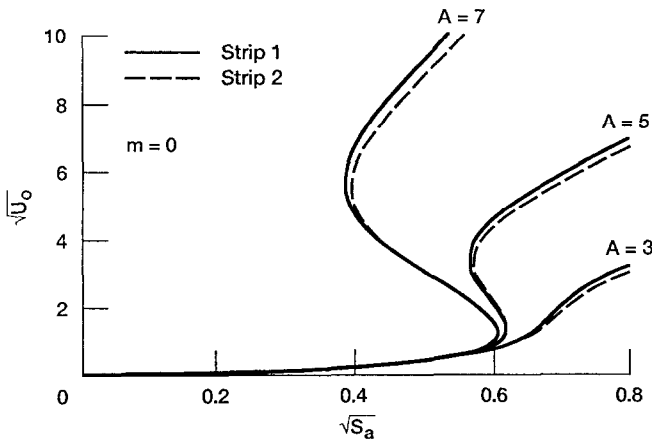
FIG. 6. Normalized crack mouth opening displacement vs normalized loading parameter for bridged edge crack under uniform tension.
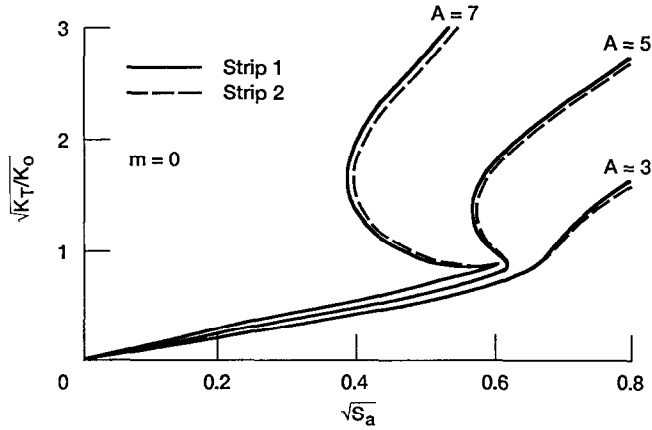
FIG. 7. Normalized total stress intensity factor vs normalized loading parameter for bridged edge crack under uniform tension.

Notice that for a bridged Griffith crack ($b = h/2$, $a/h \to 0$), the effects of free surfaces disappear, and the Fourier transform kernel $K(t, \tau)$ vanishes. Consequently, the compliance matrix C in (36) is independent of elastic moduli. As illustrated by Figs 3–5, where the Weibull modulus $m = 1$, the relations between U_0 and S_a, K_T/K_0 and S_a and K_F/K_0 and S_a are universal for all orthotropic strips with common values of A.

The stability of the bridged cracks can be viewed either through the $\sqrt{U_0}$ versus $\sqrt{S_a}$, $\sqrt{K_T/K_0}$ versus $\sqrt{S_a}$ or $\sqrt{K_F/K_0}$ versus $\sqrt{S_a}$ plots. Figure 3 shows that for relatively short cracks an increase in load is needed to increase the crack mouth opening displacement (CMOD). For long cracks, on the other hand, as the fibers start pulling out the CMOD increases even if the load is decreased. In other words, the instability is indicated by a discontinuity in the CMOD.

Consider next the stress intensity factors. Figure 5 shows that for the stable short
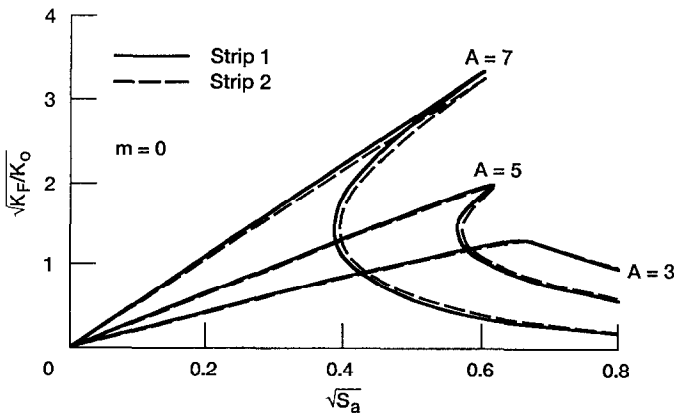
FIG. 8. Normalized shielding stress intensity factor vs normalized loading parameter for bridged edge crack under uniform tension.

cracks, the shielding produced by the fibers varies stably, while for long cracks there is a sharp reduction in shielding as the fibers pull out. This sharp reduction corresponds to the discontinuous increase in total stress intensity factor in Fig. 4.

Of interest is how the normalized quantities A and H work when the orthotropic strips have finite geometry configurations. Figures 6–8 show the curves $\sqrt{U_0}$ versus $\sqrt{S_a}$, K_T/K_0 versus $\sqrt{S_a}$ and K_F/K_0 versus $\sqrt{S_a}$ for bridged edge cracks with $m = 0$ under uniform tension. From these figures it is seen that even in finite geometries the above normalized quantities can still yield nearly universal results, regardless of the level of anisotropy. Although they are not presented here, the results for bending loading and for center cracked strips showed similar trends.

The above results suggest that the regular kernel $K(t, \tau)$ in (23) can be expressed as $K^0(t, \tau)[1 + Y(\rho, a/h, b/h)]$ where $K^0(t, \tau)$ is the regular kernel of the corresponding isotropic cracked strip and $Y(\rho, a/h, b/h)$ is a higher order perturbation term which is a function of ρ, a/h and b/h with $Y(1, a/h, b/h) = 0$ and $Y(\rho, 0, 0.5) = -1$. To obtain the detailed form of $Y(\rho, a/h, b/h)$ further numerical investigation is needed and is not discussed in this paper.

Here it should be emphasized that although in all the above calculations only the bulk moduli enter (4) and (13), for real fiber-reinforced composites the bulk moduli are related to the constituent properties. There are many procedures published in the literature to perform this homogenization process (Mura, 1987).

From the foregoing analysis it is seen that the length parameter a_n is a key parameter to define all relevant normalized quantities such as the normalized crack length A, normalized strip width H, normalized stress intensity factors K_T/K_0 and K_F/K_0. Then, what role is played by the constituent properties in determining the value of a_n? To this end, the parameter a_n is written as

$$a_n = \frac{\pi}{16} \frac{\Sigma R}{\tau} \alpha \tag{43}$$

where

$$\alpha = \frac{(1 - f) E_m E'}{f E_1 E_{11}}, \tag{44}$$

which comprehensively reflects the influence of the constituent stiffness and the fiber volume fraction on a_n.

Consider the following composite whose fibers are aligned along the x-axis with $E_f/E_m = 10$, $v_f = 0.3$ and $v_m = 0.35$ where E_f and E_m are Young's moduli of the fiber and matrix, respectively, and v_f and v_m are their Poisson's ratios. The well-known Mori–Tanaka method (Luo and Weng, 1989) was used to determine the five effective elastic constants of the composite strip. Figure 9 shows α, E'/E_m and E_{11}/E_m as functions of f for plane strain. Figure 10 plots α versus f for several values of E_f/E_m. Figure 11 shows the variation of α, E'/E_m and E_{11}/E_m with respect to E_f/E_m for $f = 0.4$. It is observed that when the volume fraction is low, α sharply decreases with an increase in f, while beyond this range α changes slowly. Besides, α decreases with increasing E_f/E_m. From the above observations it is clear that, since large values of A in general correspond to less stable bridged cracks, then for a given length of bridged
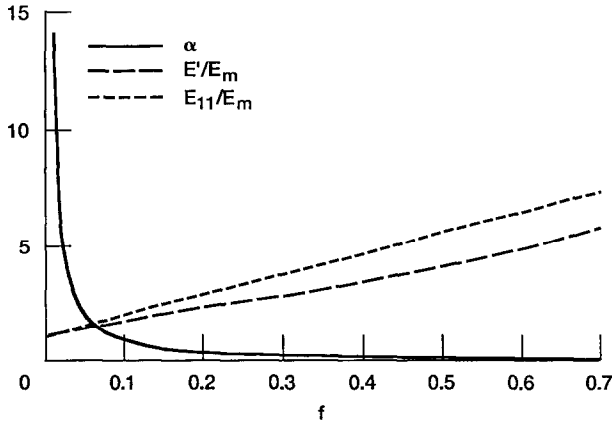
FIG. 9. Nondimensional parameters α, E'/E_m and E_{11}/E_m vs fiber volume fraction f for composite with $E_f/E_m = 10$, $v_f = 0.3$ and $v_m = 0.35$.

crack increasing the stiffness ratio E_f/E_m or volume fraction f will reduce the stability of the bridged crack. However, this can be compensated for by increasing the fiber strength Σ, fiber radius R and decreasing the interfacial frictional friction stress τ.

4. CONCLUDING REMARKS

A singular integral equation formulation has been presented for the analysis of bridged cracks in orthotropic strips. The exact solutions given in this paper show that
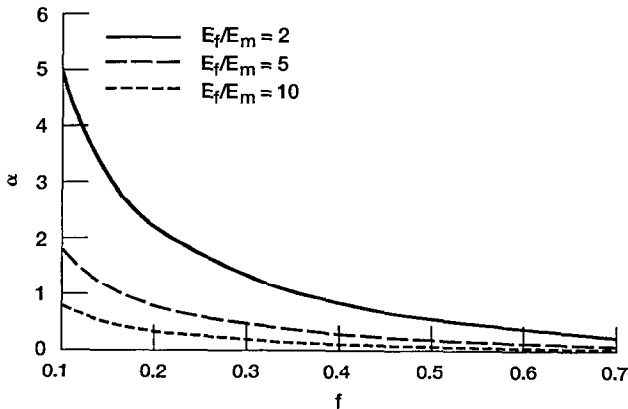
FIG. 10. Nondimensional parameter α vs fiber volume fraction f for several composites with $v_f = 0.3$ and $v_m = 0.35$.
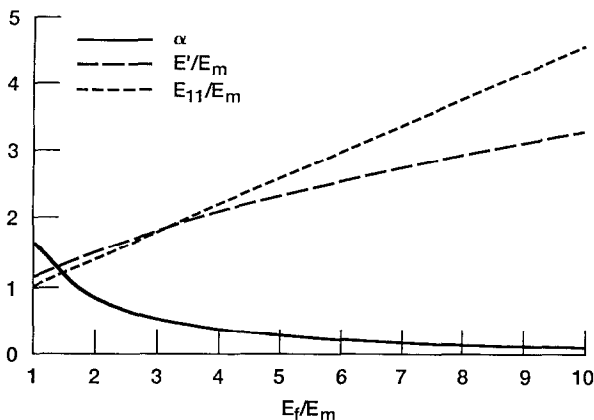
Fig. 11. Nondimensional parameters α, E'/E_m and E_{11}/E_m vs E_f/E_m for composite with $v_f = 0.3$, $v_m = 0.35$ and $f = 0.4$.

in terms of the normalized parameters introduced by Cox and Marshall (1991) the nonlinear behavior of bridged cracks can be depicted in a nearly universal form for materials possessing different levels of anisotropy. The increase of the ratio of stiffness E_f/E_m and volume fraction f in general reduces the stability of the bridged cracks, which can be remedied by increasing the fiber strength and fiber radius and decreasing the interfacial frictional friction stress.

ACKNOWLEDGEMENTS

REFERENCES

Ballarini, R. (1986) Compliance matrices for cracked bodies. *Int. J. Fracture* **31**, R63–R66.
Ballarini, R. and Muju, S. (1993) Stability analysis of bridged cracks in brittle matrix composites. *J. Engng Gas Turbines Power* **115**, 127–138.
Bao, G., Ho, S., Suo, Z. and Fan, B. (1992) The role of material orthotropy in fracture specimens for composites. *Int. J. Solids Struct.* **29**, 1105–1116.
Budiansky, B. and Amazigo, J. C. (1989) Toughening by aligned, frictionally constrained fibers. *J. Mech. Phys. Solids* **37**, 93–109.
Bueckner, H. F. (1970) A novel principle for the computation of stress intensity factors. *Z. Angewandte Mathemat. Mechan.* **50**, 529–546.
Cox, B. N. and Marshall, D. B. (1991) Stable and unstable solutions for bridged cracks in various specimens. *Acta Metall.* **39**, 579–589.
Cox, B. N. (1991) Extrinsic factors in the mechanics of bridged cracks. *Acta Metall.* **39**, 1189–1201.
Delale, F. and Erdogan, F. (1977) The problem of internal and edge cracks in an orthotropic strip. *J. Appl. Mech.* **44**, 237–242.

EVANS, A. G. (1991) The mechanical properties of reinforced ceramic, metal and intermetallic matrix composites. *Mater. Sci. Engng* **A143**, 63–76.

GERASOULIS, A. (1982) The use of piecewise quadratic polynomials for the solution of singular integral equations of Cauchy type. *Comput. Math. Appl.* **8**, 15–22.

KAYA, A. C. and ERDOGAN, F. (1980) Stress intensity factors and COD in an orthotropic strip. *Int. J. Fracture* **16**, 171–190.

LEKHNITSKII, S. G. (1981) *Theory of Elasticity of an Anisotropic Body*. Mir Publishers, Moscow.

LUO, H. A. and WENG, G. J. (1989) On Eshelby's S-tensor in a three-phase cylindrically concentric solid, and the elastic moduli of fiber-reinforced composites. *Mech. Mater.* **8**, 77–88.

MARSHALL, D. B. and COX, B. N. (1987) Tensile fracture of brittle matrix composites: influence of fiber strength. *Acta Metall.* **35**, 2607–2619.

MARSHALL, D. B., COX, B. N. and EVANS, A. G. (1985) The mechanics of matrix cracking in brittle matrix fiber composites. *Acta Metall.* **33**, 2013–2021.

MILNE-THOMSON, L. M. (1960) *Plane Elastic Systems*. Springer, Berlin.

MURA, T. (1987) *Micromechanics of Defects in Solids*. Martinus Nijhoff, Dordrecht.

SIH, G. C. and LIEBOWITZ, H. (1968) Mathematical theories of brittle fracture. *Fracture*, Vol. II (ed. H. LIEBOWITZ), pp. 67–190. Academic, New York.

SUO, Z. (1990a). Delamination specimens for orthotropic materials. *J. Appl. Mech.* **57**, 627–634.

SUO, Z. (1990b) Singularities, interfaces and cracks in dissimilar anisotropic media. *Proc. R. Soc. Lond.* **A427**, 331–358.

SUO, Z., BAO, G., FAN, B. and WANG, T. C. (1991) Orthotropy rescaling and implications for fracture in composites. *Int. J. Solids Struct.* **28**, 235–248.

APPENDIX

In (9), $B_j(\xi)$ is determined by

$$
\begin{cases}
b_{12}\xi \sum_{j=1}^{4} B_j(\xi) + b_{22}\xi \sum_{j=1}^{4} d_j s_j B_j(\xi) = f_1(\xi), \\[2mm]
G_{12}\xi \left[\sum_{j=1}^{4} s_j B_j(\xi) - \sum_{j=1}^{4} d_j B_j(\xi) \right] = f_2(\xi), \\[2mm]
b_{12}\xi \sum_{j=1}^{4} B_j(\xi)\, e^{y_j \xi h} + b_{22}\xi \sum_{j=1}^{4} d_j s_j B_j(\xi)\, e^{y_j \xi h} = f_3(\xi), \\[2mm]
G_{12}\xi \left[\sum_{j=1}^{4} s_j B_j(\xi)\, e^{y_j \xi h} - \sum_{j=1}^{4} d_j B_j(\xi)\, e^{y_j \xi h} \right] = f_4(\xi),
\end{cases}
\tag{A.1}
$$

where

$$
f_1(\xi) = -\frac{\pi i}{4}[A_1\, e^{i\lambda_1 y_0 \xi} + A_2\, e^{i\lambda_2 y_0 \xi}],
$$

$$
f_2(\xi) = \frac{\pi}{4}[A_1 \lambda_1\, e^{i\lambda_1 y_0 \xi} + A_2 \lambda_2\, e^{i\lambda_2 y_0 \xi}],
$$

$$
f_3(\xi) = -\frac{\pi i}{4}[\bar{A}_1\, e^{-i\bar{\lambda}_1(h-y_0)\xi} + \bar{A}_2\, e^{-i\bar{\lambda}_2(h-y_0)\xi}],
$$

$$
f_4(\xi) = \frac{\pi}{4}[\bar{A}_1 \bar{\lambda}_1\, e^{i\bar{\lambda}_1(h-y_0)\xi} + \bar{A}_2 \bar{\lambda}_2\, e^{i\bar{\lambda}_2(h-y_0)\xi}].
\tag{A.2}
$$